**Atmospheric
Chemistry
and Physics
Discussions**

**SDS numerical
forecast system in
Asia and its
performance**

C. H. Zhou et al.

Title Page

Abstract	Introduction
Conclusions	References
Tables	Figures

◄◄	►►
◄	►
Back	Close

Full Screen / Esc

Printer-friendly Version

Interactive Discussion

EGU

Development and evaluation of an operational SDS forecasting system for East Asia: CUACE/DUST

C. H. Zhou[1], S. L. Gong[1,2], X. Y. Zhang[1], Y. Q. Wang[1], T. Niu[1], H. L. Liu[1],
T. L. Zhao[2], Y. Q. Yang[1], and Q. Hou[1]

[1]Centre for Atmosphere Watch & Services (CAWAS), Chinese Academy of Meteorological
Sciences, China Meteorological Administration (CMA), Beijing 100081, China
[2]Air Quality Research Division, Science & Technology Branch, Environment Canada, 4905
Dufferin Street, Toronto, Ontario M3H 5T4, Canada

Correspondence to: C. H. Zhou (zhouch@cma.gov.cn)

Abstract

CUACE/Dust, an operational sand and dust storm (SDS) forecasting system for East Asia, was developed at CMA (China Meteorological Administration) by integrating a meso-scale dust aerosol model with a 3DVar data assimilation system that uses both
5 surface network observation data and dust intensity data retrieved from the Chinese Geostationary Satellite FY-2C. For spring 2006, CUACE/Dust successfully forecasted most of the 31 SDS episodes in East Asia. A detailed comparison of the modeling predictions for the 8–12 March episode with surface network observations and lidar measurements revealed a robust forecasting ability of the system. The time series of
10 the forecasted dust concentrations for a number of representative stations for the whole spring 2006 were also evaluated against surface PM10 monitoring data, showing a very good agreement in terms of the SDS timing and magnitudes near source regions where dust aerosols dominate. For the entire domain forecasts in spring 2006 (1 March–31 May), a TS (thread score) system evaluated the performance of the system against all
15 available observations and rendered an averaged TS value of 0.31 for 24 h forecasts, 0.23 for 48 h and 0.21 for 72 h forecasts.

1 Introduction

As a natural weather phenomenon, sand and dust storm plays an important role in global climate changes. Its radiative forcing is estimated to be $-0.6\sim0.4\,\mathrm{w\,m^{-2}}$ with
20 great uncertainties (IPCC, 2001). Dust storms throughout Asia, Middle East and Northern Africa are estimated to cycle more than 200 to 5000 Mt/year of mineral dust into the earth's atmosphere (Tegen and Fung, 1994) with a total emission of about 800 Mt/year from Asia alone (Zhang et al., 1997). Although with a great interannual variability (Gong et al., 2006), most Asia SDS occurs in spring time. The frequency of SDS ranges from
25 one day per year in most part of North China to about 100 days per year in places near the desert like Yan Chi (Zhou, 2001). Dust storms directly cause low atmospheric visi-

bility, thus impact the commercial and military operations and people's daily life in dust prone regions. In these regions, the surface vegetation can also be destroyed when the plants are covered with heavy mineral particles or have been blown up by strong sandy wind during SDS. Unlike coarse mineral particles which deposit in and near the source regions, finer particles are suspended in the air for a longer time and more easily transported to a place far away from the source areas. They can also take in or be taken by other chemical components like BC, OC or sulfate during the transports. These finer particles, especially with the diameter less than $10\,\mu m$, can be freely haled into human bodies to cause health problems. Some severe SDS could be a disaster like the one with visibility less than $50\,m$ occurred 5 May in 1995 in Jin Chang, Gansu province of China which caused 85 fatalities and 31 missing. To alleviate SDS impacts, a very effective way is to issue forecast and early warning information in dust prone regions.

Many attempts have been made for SDS simulations and forecasts. Those models, including NARCM (Gong et al., 2003b) from Canada, DREAM from Spain (Pe'rez et al., 2006) and CFORS (Uno et al., 2001) in Japan, have simulated SDS occurrence, transport and depositions. The model results show relatively good agreement with routine and intensified SDS observation such as satellite data, surface TSP (total suspended particle) and PM10 horizontal and vertical distributions. Because of varieties of dust emission schemes, horizontal and vertical resolutions, numerical methods, and different meteorological models, eight models from different counties show quite different performance for Asian dust episodes in March and April of 2003 in terms of flux, transport, horizontal and vertical distribution outputs in the DMIP project (Uno et al., 2006), which concluded that reliable surface land use conditions and soil/surface information are more important than the complexity of the dust emission scheme or the model horizontal resolution.

In real time SDS forecasting, it is difficult to reproduce the soil-related land surface conditions for emissions. It may make the forecasting more difficult with the bias in meteorological forecasts such as wind speed and precipitations. There are two ways to al-

leviate these shortcomings. One is to upgrade more "real-time" wind erosion database including soil size distribution, deserts distribution, soil/dust size distribution and soil water etc. Another is to establish SDS data assimilation systems with satellite and/or surface observations to improve the SDS initial condition in the numerical systems.

5   This paper presents a SDS forecasting system – CUACE/Dust (Chinese Unified Atmospheric Chemistry Environment – Dust) developed by coupling dust aerosol microphysics onto a mesoscale meteorological model with an improved SDS vertical diffusion and 3-D advection schemes at CMA. With CUACE/Dust, three-day SDS real time forecasting and early warning information has been issued in spring time from

10 March to May in East Asia since 2005. In this paper, the frame and configurations of CUACE/Dust, including the emission scheme together with a sand erosion database, improved advection and transport schemes, and a 3Dvar SDS data assimilation system, will be introduced. Then the model forecasting ability was analyzed and evaluated for the dust episodes in 2006 by comparing with surface dust and PM10 concentra-

15 tions of the CMA observation networks and vertical structure from Lidar observations of NIES of Japan. The model average forecasting ability was also analyzed in the entire domain by a SDS scoring system with TS scores, misses, false alarms and forecast accuracy developed at CMA.

2   Description of CUACE/Dust

20 CUACE has been designed as a unified chemistry module which can be easily coupled onto any atmospheric models at various temporal and spatial scales. It compasses a chemistry interface for tracers of aerosols and gases, which passes the atmospheric backgrounds like wind, temperature and humidity together with model configurations into the chemistry module to calculate the chemical/physical processes for the trac-

25 ers. The chemical fields can also be fed back into the host model for aerodynamic processes like diffusion and advection and post analysis through the interface. The chemistry module for aerosols in CUACE is a size-segregated multi-component algo-

rithm for all types of aerosols such as dust, sea salt, BC/OC, sulfate, nitrate and ammonium (Gong et al., 2003a). It includes major aerosol processes in the atmosphere such as the generation, hygroscopic growth, coagulation, nucleation, condensation, dry depositions, scavenging and aerosol activations.

2.1 Dust aerosol in CUACE

CUACE/Dust forecasting system was developed based on a size-segregated dust aerosol module of CAM (Canadian Aerosol Module) (Gong et al., 2003a) that was coupled into a mesoscale meteorological model – MM5 to conduct real time SDS forecasting in Northeast Asia. A positive 3-D advection scheme called MPDATA has also been introduced and an anti-gradient diffusion scheme has been developed in the system for dust advection and diffusion processes, respectively.

In CUACE/Dust, all the atmospheric processes are included except for the coagulation and nucleation which are not important for mesoscale SDS simulation and forecasting. Particle size distribution plays a great role in aerosol microphysics and large scale transport processes. Studies (Zhang et al., 2003) show that the dominant mass of the mineral aerosols in Northeast Asia was with diameters from 2 to 20 μm which accounts for about 53%–68% of the total mineral dust loading. It may shift slightly to course mode in heavy dust storms near the source regions and to fine mode in receptor regions. Based on the Zhang's studies, the mineral aerosol size spectra in CUACE/Dust are divided into 12 size bins with a radius range of 0.02–0.04, 0.04–0.08, 0.08–0.16, 0.16–0.32, 0.32–0.64, 0.64–1.28, 1.28–2.56, 2.56–5.12, 5.12–10.24, 10.24–15.36, 15.36–17.36, 17.36–20.72, 20.72–30 μm.

2.2 Dust emission schemes and erosion database

There are two dust emission schemes built in CUACE/Dust: (1) by Marticorena and Bergametti (1995), Alfaro et al. (1997), Alfaro and Gomes (2001) (hereinafter referred to as MBA) and (2) by Shao (2001, 2004). Both of these schemes require a com-

ACPD

7, 7987–8015, 2007

SDS numerical forecast system in Asia and its performance

C. H. Zhou et al.

Title Page

Abstract | Introduction

Conclusions | References

Tables | Figures

◄ | ►

◄ | ►

Back | Close

Full Screen / Esc

Printer-friendly Version

Interactive Discussion

prehensive soil erosion database, which includes deserts and semi-deserts distributions, soil grain-size, soil moisture content, snow cover, landuse and surface roughness length. For East Asia, parameters and data sets to drive these two schemes have been derived and compared (Zhao et al., 2006) . In current CUACE/Dust, the MBA scheme is used. A detailed desert distribution and soil texture data base for China was given in (Gong et al., 2003b). The snow cover was retrieved from NOAA17 AVHHR at the resolution of $0.02° \times 0.02°$.

2.3 The host model – MM5

For the 2006 forecasting season, a nonhydrostatic version of MM5 was used as the meteorological driver to host CUACE/Dust. Its horizontal dimensions are set to be 68×85 at a resolution of 108 km and the number of vertical sigma-levels is 24 with the sigma value for each level as 1.0, 0.996, 0.992, 0.986, 0.980, 0.970, 0.955, 0.930, 0.900, 0.860, 0.810, 0.760, 0.710, 0.660, 0.600, 0.530, 0.460, 0.390, 0.320, 0.250, 0.180, 0.110, 0.050 and 0. Ten days of meteorological forecasts from T213, an operational global medium range spectrum meteorological model with the resolution of $0.625°$, are interpolated to formulate the meteorological initial, boundary and lateral conditions for MM5.

The key parameters from a host model that can significantly influence the performance of CUACE/Dust are the 3-D winds, boundary-layer turbulence, surface fluxes, cloud and precipitation as well as the soil moisture contents. They determine not only the production of dust aerosol but also its long-range transports.

There are a number of improvements done to provide more reasonable parameters to drive the dust forecasts. In CUACE, a Multi-dimensional Positive Definite Advection Transport Algorithm (MPDATA) (Smolarkiewicz, 2006) has been introduced as the advection scheme for all tracers. It is based on the upstream differential scheme and was proposed firstly as a simple positive-definite advection scheme with small implicit diffusion for the advection of water-substance constituent in atmospheric cloud models. A nonscillatory option can also be applied to this scheme to assure monotonicity.

It is stable, consistent and conservative for positive definiteness. Vertical diffusion in sub-grid scale is often another important progress controlling the transports of tracers to the upper layer and to downwind regions. A nonlocal vertical diffusion scheme has been adopted in CUACE which is an improved approach from local-k method based on local gradients of wind and potential temperature with the deficiencies for highly unstable conditions where the local gradients can not model the transport by large eddies representing the bulk property of the whole PBL (Hong and Pan, 1996).

2.4 Data assimilation system for CUACE/Dust

One of the unique features of CUACE/Dust system is the implementation of a three dimensional data assimilation module that combines the observations of the surface monitoring networks with FY-2C SDS retrieval data (Hu et al., 2007; Niu et al., 2007). The assimilated dust concentrations have been updated as the model initial conditions everyday in the forecasting system.

2.5 Threat Score (TS) system for CUACE/Dust

A TS scoring system has been established to verify the model's performance. The observation for the evaluation merges the satellite retrieval information, surface synoptic observation and PM10 network in CMA (Wang et al., 2007[1]). It can give out the verification information of threat score, misses, false alarm ratio and accuracy for different forecast length at each mesh of the domain for the forecast system

---

[1]Wang, Y. Q., Zhang, X. Y., Gong, S. L., Zhou, C. H., Hu, X. Q., Liu, H. L., Niu, T., and Yang, Y. Q.: Surface observation of sand and dust storm in East Asia and its application in CUACE/Dust forecasting system, Atmos. Chem. Phys. Discuss., submitted, 2007.

3   Results and evaluation

Forecasting results for spring 2006 were evaluated and compared with available observation data across East Asia. For a detailed description of the Chinese network observations during this period, one can refer to a companion paper (Wang et al.,

5   2007[1]) of this special issue. Analysis of synoptic weather patterns associated with the dust storms for spring 2006 was also investigated, which defined the SDS process according to certain criteria (Yang et al., 2007).

There were 31 SDS episodes occurred from 1 March to 31 May in 2006 in Northeast (NE) Asia, among which 13 were Severe SDS, 12 were SDS and 6 were Blowing Dust

10   (Table 1). For all the SDS episodes, 5 most striking and notorious severe SDS events hit large regions and caused great damages in NE Asia, 10 transported to Beijing and 8 to Korean Peninsula and 3 to Japan Islands. The episodes 8–12 March was among the most striking ones which also hit Beijing, Korea peninsula and even to Japan. Because of its heavy extensity, magnitude, and long persistency, the case 8–12 March

15   has been chosen to evaluate the CUACE/Dust's performance on dust emission, vertical distribution and long-range transport in the real time forecasting.

Besides the synoptic data and Chinese network observations (Wang et al., 2007[1]), Lidar observation of back scattering intensity and depolarization ratio in every 15 min from a lidar observation network (http://www-lies.lidar.go.jp) of 10 stations were also

20   used to compare with the forecasting results. These stations mostly located in NE Asia for dust aerosol vertical distribution research since 2001 .(Sugimoto et al., 2000). Five stations named Shapotou (104.95° E, 37.46° N), Huhhot (111.4° E, 40.9° N), Beijing (116.17° E, 39.56° N), Seoul (126.59° E, 37.34° N) and Tsukuba (140.12° E, 36.05° N) from the network have been selected for vertical dust distribution comparison, rep-

25   resenting the regions of the deserts, near source areas and downwind of the SDS transport in NE Asia.

3.1 Dust episode of 8–12 March 2006

Synoptic records show that during 8–12 March, a severe extensive SDS stroke Mongolia, Northwest, North and Northeast China, Korea Peninsula, and Japan (Yang et al., 2007). It started at 14:00 (BST) on 8 March in Mongolia, hit China massively from 9 March and ended at 02:00 (BST) on 12 March in Korea Peninsula. SDS phenomena have been observed in Mongolia and many places in North China such as Inner Mongolia, Qinghai, Gansu, Ningxia, Shaanxi, Shanxi and Liaoning provinces. The black SDS phenomena have been observed in two stations: Zhurihe and Suniteyouqi, with zero visibility and wind speed exceeding 20 m/s and in 3 other stations nearby with visibility less than 100 m in the area of Onqin Daga Sand Areas in the afternoon on 9 March. This severe SDS episode is the first and one of the strongest SDSs hit Northeast Asia in 2006.

Three 72 hrs real time forecasts started at 00:00 Z of 6–8 March by CUACE/Dust successfully captured the 14 h onset of 8 March SDS originated from the west of Mongolia where a cold air mass has swept to produce a severe SDS event. This is clearly shown from the agreements between the surface dust reports observed in this region and the surface dust concentration centers from the model predictions at different forecast lengths (54 h, 30 h and 6 h) (Fig. 1). Forecasting the onset of a dust episode requires a good prediction of location and strength of the surface wind speeds and soil surface conditions. Dust emission has an apparent diurnal cycle in the source areas, beginning in the morning and reaching the maximum in the afternoon and weakening thereafter. Both forecasts and observations indicated that this dust episode has not reached the class of Severe SDS until 14:00 (BST) in the afternoon on 9 March.

As the dust episode progressed, the SDS centre moved in southeast direction and its covering area increased. Figure 2 shows the 54 h, 30 h and 6 h forecast results for 14:00 (BST) of 9 March with surface SDS observations, starting at 00:00 Z of 7, 8 and 9 March. All the three forecasted results show that the SDS concentrated in the region of south of Mongolia and Inner Mongolia of China, agreeing to the surface

SDS observation with severe SDS, SDS and blowing dust observed in many stations over these regions. The 30 hrs forecasts were a little better than those of 54 h by good performance in the SDS region in and near China. The 6 h forecast was the best both in intensity and in coverage in these regions by covering all the SDS observation and without misses or false alarms when compared with the surface observation. For this 6 h forecast, there were three high concentration centers. One was located at the Badain Juran, Tengger and Ulan Buh Deserts in the west of Inner Mongolia with the highest value over $20\,000\,\mu g\,m^{-3}$. The observed PM10 reached its peak of $6600\,\mu g\,m^{-3}$ in Ejilaqi, a station in the northwest edge of Badain Juran. Another centre was in Onqin Daga sand areas in the east of Inner Mongolia with the highest predicted value over $20\,000\,\mu g\,m^{-3}$ as the observed PM10 of over $6600\,\mu g\,m^{-3}$ in Zhurihe, a station in the west edge of Onqin Daga sand areas. The third one was in Middle Gobi of Mongolia with the highest forecasted value over $10\,000\,\mu g\,m^{-3}$.

Six hours later (9 March, 20:00 BST), the main body of the dust episode moved into China and covered most part of Inner Mongolia and part of Shaanxi, Shanxi, Hebei and Liaoning provinces. The 60 h, 36 h and 12 h forecasts agreed reasonably with the surface records in and near the source areas with a missing forecast in the Onqin Daga sandy areas by the 60 h output (Fig. 3). One reason for this missing forecast is that the forecasted cold air mass along with Mongolian Cyclone has not reached there yet and located only in the west part of Inner Mongolia. Another reason is that there is a less emission in the upstream Mongolia in previous prediction which causes less dust transported to this area. The other two (36 h and 12 h forecast) have forecasted the cold air-mass with the Mongolian Cyclone correctly.

Forecasting the long-range transports of SDS is critical in providing the public enough time to reduce the damages of the SDS. From the observations, this episode covered the downwind areas in east and north part of China, Korea Peninsula and Japan islands after three days from the onset. Figure 4 shows the model results forecasted at 00:00 Z of 9 March for this long range transport. At 14:00 (BST) in the afternoon of 10 March, the forecasted surface concentration caught the SDS records

in the west of Inner Mongolia which illustrated a new emission in this area while the front of the SDS has reached Liaoning, Bohai sea, Shangdong, Hebei, Henan, Shanxi Provinces at the moment. At 20:00 (BST) in the evening, the dust belt has moved to North Korea which was agreed by the surface observations. At 14:00 (BST) in the afternoon of 11 March, part of the dust belt still stayed in the area of Shanxi, Henan, Jiangsu in China with suspended dust and haze observed in the stations over there. Another part of the dust belt has reached South Korea where there were suspended dusts observed in many stations. At 02:00 (BST) in the early morning of 12 March, there were a few suspended dusts observed in southern end of South Korea, where the forecasted dust belt was about to move out of this area.

Like the conventional weather forecasts, the forecast length accounts for the forecast difference and accuracy in dust concentration and meteorology and the influence of the initial assimilated SDS data. Generally speaking, shorter forecast length yielded a better result than longer forecast time. This is partially due to the ability of a meso-scale model to accurately predict the meteorology as a function of time. Another reason for the difference comes mainly from the impact of SDS data assimilation. In CUACE, a 3DVAR system has assimilate the near real-time SDS data from surface SDS records and satellite retrieval SDS Infra-red differential Dust Index (SDS-IDDI) into the model to provide the initial SDS conditions. As the impact of 3Dvar initial conditions weakening, the wind filed plays a dominant role on the dust emission and transport. Due to this reason, both of the outputs of 36 h and of 12 h have quite correctly forecasted the surface dust distribution and have little difference to each others (Fig. 3). More real SDS information and shorter time lag means more impact on SDS distribution which was exactly true for the case with the initial forecasting time of 00:00 Z on 9 March. Because of more surface and satellite observation information added into the model, the dust concentration and distribution show much better than the other two with initial forecasting time of 00:00 Z on 7 March and on 8 March where little SDS observation information was available to be assimilated into the model prediction.

TS of this dust episode is 0.55, 0.34 and 0.29 for 24 h, 48 h and 72 h forecast which

is much higher than the spring average value of about 0.31, 0.23 and 0.21 respectively. The forecasting efficiency is 0.89, 0.85 and 0.84 for 24 h, 48 h and 72 h forecast.

To further explore the performance of CUACE/Dust, the time-height sectional plots for this dust episode were compared with lidar observations at four stations of Shapotou, Huhhot, Beijing and Tskuba (Fig. 5). For Shapotou, a station in the south of Badain Juran Deserts, the predicted peak concentrations were in the layer under 1000 m, from 11:00 (BST) in the morning to 20:00 (BST) in the evening at each day from 9 March to 12 March and close to 5000, 10 000 and 1000 μg m^{-3} respectively. This agrees with the lidar vertical profile observations in the station. Both the forecast and the observation have a diurnal cycle which starts at about 11:00 (BST), reaches the maximum at about 14:00 (BST) in the afternoon and weakens to 20:00 (BST). For Huhhot, a station to the east of Badain Juran Deserts areas, the forecasted concentration peak of 10 000 μg m^{-3} on 9 March starting from 11:00 (BST) to 20:00 (BST) was located under 3000 m and agreed well with the lidar observation. On 10 March, the daytime concentration peak with a value of 1000 μg m^{-3}was much weaker than that of the previous day, matching to the Lidar observation.

For Beijing, both model predictions and lidar observations showed that the dust storm was transported to it through the upper air and settled down to the surface at about 19:00 (BST) in the evening. The dust concentration center located at 2000–3000 m in altitude. For Tsukuba in Japan, the dust transported to its upper air over with a much lower concentration of 500 μg m^{-3} from the forecasts at a height of about 1000–6000 m after 20:00 (BST) on 11 March when it was also the ending time of this dust episode from the surface weather stations on SDS. The relative strength and plume height of the time series were also monitored by the lidar.

The comparison in these four stations illustrates that CUACE/Dust has a good performance for the timely forecasts of dust storm arrival at most East Asian stations. This reflects the well developed micro-physical and metrological dynamic processes in the CUACE/Dust system to treat the dust emission in the source areas, vertical diffusion and horizontal transports to the downwind areas.

EGU

3.2 Surface station comparisons

During the spring 2006, the SDS monitoring network was operating and measuring the PM10 concentrations in a number of stations (Wang et al., 2007[1]). Five of them, representing the source regions at Tazhong, Ejilaqi and Zhurihe, and the downwind areas at Beijing and Dalian, were chosen to evaluate the forecasting performance of CUACE/Dust system.

Five SDS episodes: DS5, DS16, DS26, DS27 and DS29 (Table 1 and Fig. 6a) were observed in Tazhong of the Takilimakan Deserts during spring 2006. For the severe SDS episode of DS5 on 12 March, all three forecasts (FT1, FT2 and FT3) have predicted this episode. Comparing to the observed daily mean PM10 of 5011 μg m^{-3} for this case, the forecasted total dust concentrations by three consecutive predictions had a mean daily average value of 4571 μg m^{-3}, 3538 μg m^{-3} and 1023 μg m^{-3}, respectively, under-estimating the concentrations even though the model has a dust size spectrum of 40 μm. In another severe SDS episode DS16, all three FTs have forecasted the SDS episode and the concentration peaks too. FT1 forecasted a total dust concentration of 7363 μg m^{-3} which is rather comparable to the observed PM10 concentration of 6467 μg m^{-3}.

For the total five dust episodes, the forecasted surface dust concentrations are in a general good agreement with the trends of PM10 observations. The 24 hrs average (FT1) is closer to the observed PM10 concentrations with minor under-prediction while the under-estimates for FT2 and FT3 were much higher. For local small dust events in Tazhong, the model also shows good result as to the concentration trend like day 16, day 26–29 and day 51–55. FT1 shows a little better performance than FT2 and FT3 in these days but the difference of these three mean values is not so significant as that in the SDS episodes.

Ejilaqi in the Badain Juran deserts recorded thirteen dust episodes during spring 2006 as shown in Fig. 6b. The time series forecasted by FT1, FT2 and FT3 agree very well with those of PM10 observations in terms of both the time of each dust storm

Title Page

Abstract | Introduction

Conclusions | References

Tables | Figures

◀◀ | ▶▶

◀ | ▶

Back | Close

Full Screen / Esc

Printer-friendly Version

Interactive Discussion

and concentrations except for DS19 with a gap of about $100\,\mu\mathrm{g\,m^{-3}}$ by FT1. These illustrate that CUACE/Dust performed much better in dust concentration magnitude at Ejilaji than that at Takilimakan Deserts.

There were also thirteen dust episodes occurred at Zhurihe, a station in the west of Onqin Daga sandy areas (Fig. 6c) in the east of Inner Mongolia, in spring 2006. Like the case of Ejilaqi, forecasting results matched reasonably well with the PM10 observations at this station. FT1 shows under-predictions in six cases of DS 4, DS 7, DS 9, DS 17, DS 28 and DS 29 and does much better than FT2 and FT3 in the first four cases but worse in the last two. As the surface concentration of Zhurihe is controlled by both local emissions and transports from the upstream arid areas in Mongolia, the under-estimates might indicate some weakness in CUACE/Dust system in accurately predicting local emissions in this source areas or long-range transports from Mongolia.

Nine SDS events to Beijing were recorded in spring of 2006 (Fig. 6d). Predicted dust concentrations were smaller than those of PM10 observation in six SDS cases, i.e. DS 4, DS 7, DS 9, DS 13, DS 19 and DS 28. The mean values for FT1, FT2 and FT3 were 56, 44, $34\,\mu\mathrm{g\,m^3}$ respectively while the spring mean value for PM10 was $172\,\mu\mathrm{g\,m^{-3}}$. Most part of the surface dust particles in Beijing were transported from the source areas north or northwest to Beijing through Inner Mongolia during dust events. Zhao et al. (2003) indicated that most coarse mineral particles deposit in the source regions, and the dust particles to Beijing are largely corresponding to a 1–$3\,\mu m$ diameter range. The gap between surface SDS concentration and PM10 should be smaller than that at Tazhong, Zhurihe and Ejilaqi stations located in and near to the source areas. Besides the long-range transport, the larger gap may be explained by the location of Beijing where the PM10 observation contains much local non-dust particle pollutants with an annual average of about $142\,\mu\mathrm{g\,m^{-3}}$ (Beijing-EPA, 2006). Another reason accounts for the gap is the local dust emission because most SDS events to Beijing are accompanying with heavy winds for dust emission when most land surface is still barren in spring time.

Six SDS events intruded Dalian in 2006 spring time, i.e. DS 4, DS 9, DS 13, DS

20, DS 22 and DS 28. Similar to the case of Beijing, the time series of FT1, FT2 and FT3 are reasonably coherent to those of the PM10 observation while all the 6 cases are under predicted with DS 28 missed. The biggest gap is about 419 μg m^3 in DS 4 without considering the average PM10 concentration of about 100–150 μg m^3 in a day of no dust event by local aerosol contributions (Air pollution Annual report from EPA). FT1 did much better than that of the FT2 and FT3 during the former 4 dust events with much less under-estimates. FT2 shows relatively apparent signs of concentration peak in the former 5 dust events while its daily mean concentration is below 70 μg m^3 except for one exceeding 100 μg m^3 in DS20. FT3 with a daily average concentration of less than 30 μg m^{-3} presents much weaker signs of concentration peaks in all of these cases.

3.3 TS of spring 2006

To fully evaluate the overall performance of the CUACE/Dust forecasting results for spring 2006, a TS scoring system was developed (Wang et al., 2007[1]) to compute the threat score (TS), miss ratio (MR), false alarm ratio (FAR), and bias score (BS) and accuracy (AC) for the whole model domain or part of the domain from available observations. The average TS value which is sensitive to hits and penalizes both misses and false alarms from 1 March to 31 May in 2006 is 0.31 for FT1 and decreases to 0.23 for FT2 and and 0.21 for FT3 forecasts, respectively (Table 2). CUACE/Dust performed better for dust episodes than for other days (Fig. 7). Likewise, BS also decreases from 1.45 to 1.09 which means the model false alarm is small and decreases with the forecast length (BS>1 means false alarm dominant, and BS>1.5 means heavy false alarm dominant), while MS and FAR goes up correspondently as the forecast length increases. The accuracy is almost the same for these three forecast lengths and varies little in the entire spring (Fig. 7) which demonstrates that the model performance is stable in the whole spring.

Title Page

Abstract Introduction

Conclusions References

Tables Figures

◄ ►

◄ ►

Back Close

Full Screen / Esc

Printer-friendly Version

Interactive Discussion

EGU

4 Conclusions

CUACE/Dust, an operational SDS forecasting system with a 3Dvar data assimilation system, is utilized for the 2006 spring SDS forecasts in East Asia. Its robust forecast ability has been demonstrated for predicting a heavy SDS episode in 8–12 March by
comparing with the surface concentrations and synoptic SDS records. CUACE/Dust successfully captured the production and evolution of this episode in East Asia. Comparisons with the surface lidar measurements indicated that the model also reasonably simulated the vertical structure of SDS during this episode.

For other SDS episodes in spring 2006, time series of model predictions for DM40
were evaluated against PM10 observations at 5 representative stations. It is shown that the model was able to catch almost all the dust events occurred even with local dusty days although with some under-estimates in Takalimakan and Onqin Daga sandy areas. The forecasting system's entire behaviour has verified by a TS scoring system as well and the spring average threat score is 0.31, 0.23 and 0.21 with the average bias
score is 1.45, 1.23 and 1.09 for 24 h, 48 h and 72 h forecast. The TS score for episode 8–12 March is 0.55, 0.34 and 0.29 for 24 h, 48 h and 72 h forecast respectively.

For more accurate forecast, more work should be done to upgrade the soil-related parameters, micro-physics and circulation with regards to the dust emission and the dust driver, meteorological fields forecast. There is also some work that should be
done as to the SDS observation, especially to the vertical observation which are rare but vital to model initializations and verifications.

Title Page

Abstract | Introduction

Conclusions | References

Tables | Figures

◄◄ | ►►

◄ | ►

Back | Close

Full Screen / Esc

Printer-friendly Version

Interactive Discussion

EGU

References

Alfaro, S. C., Gaudichet, A., Gomes, L., and Maillé, M.: Modeling the size distribution of a soil aerosol produced by sandblasting, J. Geophys. Res., 102, 11 239–11 249, 1997.

Alfaro, S. C. and Gomes, L.: Modeling mineral aerosol production by wind erosion: Emission intensities and aerosol size distribution in source areas, J. Geophys. Res, 106, 18 075–18 084, 2001.

Beijing-EPA. Annual report of Environment in Beijing. (in Chinese), 2006.

Gong, S. L., Barrie, L. A., Blanchet, J.-P., Salzen, K. v., Lohmann, U., Lesins, G., Spacek, L., Zhang, L. M., Girard, E., Lin, H., Leaitch, R., Leighton, H., Chylek, P., and Huang, P.: Canadian Aerosol Module: A size-segregated simulation of atmospheric aerosol processes for climate and air quality models 1. Module development, J. Geophys. Res. 108, 4007, doi:10.1029/2001JD002002, 2003a.

Gong, S. L., Zhang, X. Y., Zhao, T. L., McKendry, I. G., Jaffe, D. A., and Lu, N. M.: Characterization Of Soil Dust Distributions In China And Its Transport During ACE-ASIA 2. Model Simulation and Validation, J. Geophys. Res., 108, 4262, doi:10.1029/2002JD002633, 2003b.

Gong, S. L., Zhang, X. Y., Zhao, T. L., Zhang, X. B., Barrie, L. A., McKendry, I. G., and Zhao, C. S.: A simulated climatology of Asian dust aerosol and its trans-Pacific transport. Part II: Interannual variability and climate connections, J. Climate, 19, 104–122, 2006.

Hong, S.-Y. and Pan, H.-l.: Nonlocal Boundary Layer Vertical Diffusion in a Medium-Range Forecast Model, Monthly Wea. Rev., 124, 2322–2339, 1996.

Hu, X. Q., Lu, N. M., Niu, T., and Zhang, P.: Operational Retrieval of Asian Dust Storm from FY-2C Geostationary Meteorological Satellite and its Application to real time Forecast in Asia, Atmos. Chem. Phys. Discuss., accepted, 2007.

IPCC: Climate Change 2001: The Scientific Basis, Contribution of working Group I to the Third Assessment Report of the Intergovernmental Panel on Climate Change. Cambridge University Press, 2001.

Marticorena, B. and Bergametti, G.: Modeling the atmospheric dust cycle. Part 1: Design of a soil-derived dust emission scheme, J. Geophys. Res., 100, 16 415–16 430, 1995.

Niu, T., Gong, S. L., Zhu, G. F., Liu, H. L., Hu, X. Q., Zhou, C. H., Wang, Y. Q., and Zhang, X. Y.: Data Assimilation of Dust Aerosol Observations for CUACE/Dust Forecasting System, Atmos. Chem. Phys. Discuss., in press, 2007.

Pe'rez, C., Nickovic, S., Baldasano, J. M., Sicard, M., Rocadenbosch, F., and Cachorro,

V. E.: A long Saharan dust event over the western Mediterranean: Lidar, Sun pho-
tometer observations, and regional dust modeling, J. Geophys. Res., 111, D15214,
doi:10.1029/2005JD006579, 2006.

Shao, Y.: A model for mineral dust emission, J. Geophys. Res., 106, 20 239–20 254, 2001.

5 Shao, Y.: Simplification of a dust emission scheme and comparison with data. J. Geophy. Res.,
109(D17), doi:10.1029/2003JD004372, 2004.

Smolarkiewicz, P. K.: Multidimensional positive definite advection transport algorithm: An
overview. International journal for numerical methods in fliuds, 50, 1123–1144, 2006.

Sugimoto, N., Matsui, I., Liu, Z., Atsushi Shimizu, Tamamushi, I., and Asai, K.: Observation of
10 Aerosols and Clouds Using a Two-Wavelength Polarization Lidar during the Nauru99 Exper-
iment. Sea and Sky 76, 93-98, 2000.

Tegen, I. and Fung, I.: Modeling of mineral dust in the atmosphere: Sources, transport, and
optical thickness, J. Geophys. Res., 99, 22 897–22 914, 1994.

Uno, I., Amano., H., Emori, S., Kinoshita, N., Matsu., I., and Sugimoto, N.: Trans-Pacific yellow
15 sand transport observed in April 1998: Numerical simulation, J. Geophys. Res., 106, 18 331–
18 344, 2001.

Uno, I., Wang, Z., Chiba, M., Chun, Y. S., Gong, S. L., Hara, Y., Jung, E., Lee, S.-S., Liu, M.,
Mikami, M., Music, S., Nickovic, S., Satake, S., Shao, Y., Song, Z., Sugimoto, N., Tanaka,
T., and Westphal, D. L.: Dust model intercomparison (DMIP) study over Asia: Overview, J.
20 Geophys. Res., 111, D12213, doi:10.1029/2005JD006575, 2006.

Yang, Y. Q., Hou, Q., Zhou, C. H., Liu, H. L., Wang, Y. Q., and Niu, T.: A Study on Sand/dust
Storms over Northeast Asia and Associated Large-Scale Circulations in Spring 2006, Atmos.
Chem. Phys. Discuss., accepted, 2007.

Zhang, X. Y., An, Z. S., and Cao, J. J.: Dust emission from Chinese desert sources linked to
25 variations in atmospheric circulation, J. Geophys. Res., 102, 28 041–28 047, 1997.

Zhang, X. Y., Gong, S. L., Shen, Z. X., Mei, F. M., Xi, X. X., Liu, L. C., Zhou, Z. J., Wang,
D., Wang, Y. Q., and Y. Cheng. Characterization Of Soil Dust Distributions In China And
Its Transport During ACE-ASIA 1. Net Work Measurements, J. Geophys. Res., 108, 4261,
doi:10.1029/2002JD002632, 2003.

30 Zhao, T. L., Gong, S. L., Zhang, X. Y., Abdel-Mawgoud, A., and Shao, Y. P.: An assessment of
dust emission schemes in modeling east Asian dust storms, J. Geophys. Res., 111, D05S90,
doi:10.1029/2004JD005746, 2006.

Zhao, T. L., Gong, S. L., Zhang, X. Y., and McKendry, I. G.: Modelled size-segregated wet and

Title Page

Abstract | Introduction

Conclusions | References

Tables | Figures

◁ | ▷

◀ | ▶

Back | Close

Full Screen / Esc

Printer-friendly Version

Interactive Discussion

dry deposition budgets of soil dust aerosol during ACE-Asia, 2001: Implications for Trans-Pacific Transport, J. Geophys. Res., 108, 8665, doi:10.1029/2002JD003363, 2003.

Zhou, Z. J.: Blowing-sand and sandstorm in China in recent 45 years, Quaternary Res. (Chinese), 21, 9–17 (in Chinese), 2001.

SDS numerical forecast system in Asia and its performance

C. H. Zhou et al.

Title Page

Abstract | Introduction

Conclusions | References

Tables | Figures

◄ | ►

◄ | ►

Back | Close

Full Screen / Esc

Printer-friendly Version

Interactive Discussion

EGU

Table 1. Dust Events in 2006 from March to May.

DS Number	Date (MM.DD-DD)	Class	Influenced Regions
1	3.3-4	SDS	Mongolia, West of Inner Mongolia
2	3.6-6	SDS	Center and SE of Mongolia
3	3.7–7	Blowing Dust	South West of Mongolia
4	3.8–12	Severe SDS	Mongolia, NW, N, NE of China, Korea Peninsula, and Japan
5	3.11–13	Severe SDS	Taklimakan basin
6	3.15–15	Blowing Dust	Onqin Daga
7	3.16–19	Blowing Dust	Mongolia, NW, N, NE of China,
8	3.21–21	Blowing Dust	S of Mongolia, West of InnerMongolia and Ningxia Province of China
9	3.23–25	Blowing Dust	Mongolia , West and Central of Inner Mongolia, N and NE China, Korea Peninsula
10	3.26–28	Severe SDS	Mongolia , West and Central of Inner Mongolia, N and NE and Central China, Korea Peninsula
11	3.29–4.1	SDS	Monggolia, Central of Inner Mongolia, NW China
12	4.1–3	SDS	Mongolia
13	4.5–9	Severe SDS	Center and South Mongolia, NW, N and NE China, Korea Peninsula and Japan
14	4.8–9	SDS	W and SE of Mongolia, Centre of Inner Mongolia
15	4.9–11	Severe SDS	West of Mongolia, NW, N and NE of China
16	4.9–20	Severe SDS	Xinjiang of China
17	4.12–13	Blowing dust	Mongolia
18	4.14–15	Blowing dust	SW of Mongolia, NW and N of China
19	4.15–19	Severe SDS	Mongolia, NW, N NE of China, Korea Peninsula and Japan
20	4.20–25	Severe SDS	Mongolia, NW, N NE of China, Korea Peninsula and Japan
21	4.24–25	SDS	West of Mongolia, NW and West of Inner Mongolia of China
22	4.28–5.1	SDS	Mongolia, NW, N NE of China, Korea Peninsula and Japan
23	5.2–4	Severe SDS	Mongolia, part of West Inner Mongolia of China
24	5.5–6	SDS	South and East of Mongolia, East of Mongolia and NE of China
25	5.8–8	SDS	Mongolia
26	5.8–9	Blowing dust	Taklimakan basin of Xinjiang
27	5.10–11	SDS	Taklimakan basin of Xinjiang
28	5.15–17	Severe SDS	Mongolia, NW, N and NE of China
29	5.19–20	SDS	Mongolia, NW of China
30	5.23–24	Severe SDS	Centre and South of Mongolia
31	5.29–30	Severe SDS	Mongolia and Inner Mongolia

Table 2. Mean TS Scoring for CUACE/Dust in 2006 Spring Time.

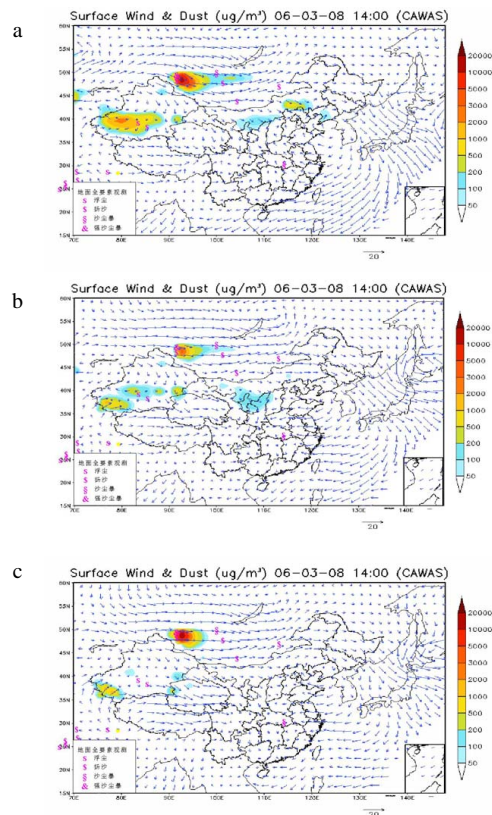| Forecast Length	0–24 h	24–48 h	48–72 h
threat score	0.31	0.23	0.21
miss ratio	0.48	0.62	0.65
false alarm ratio	0.55	0.6	0.6
bias score	1.45	1.23	1.09
accuracy	0.88	0.87	0.87

Fig. 1. Surface snap SDS concentrations and wind field at 14 h on 8 March at forecast length of **(a)** 54, **(b)** 30 and **(c)** 6 h from the initial forecast time of 8 h on 6, 7 and 8 March, respectively (Beijing standard time used). The scattered pink signals S, $, § and & represent observation records of suspended dust, blowing dust, SDS and severe SDS respectively from weather stations at the same time with the concentration plot.
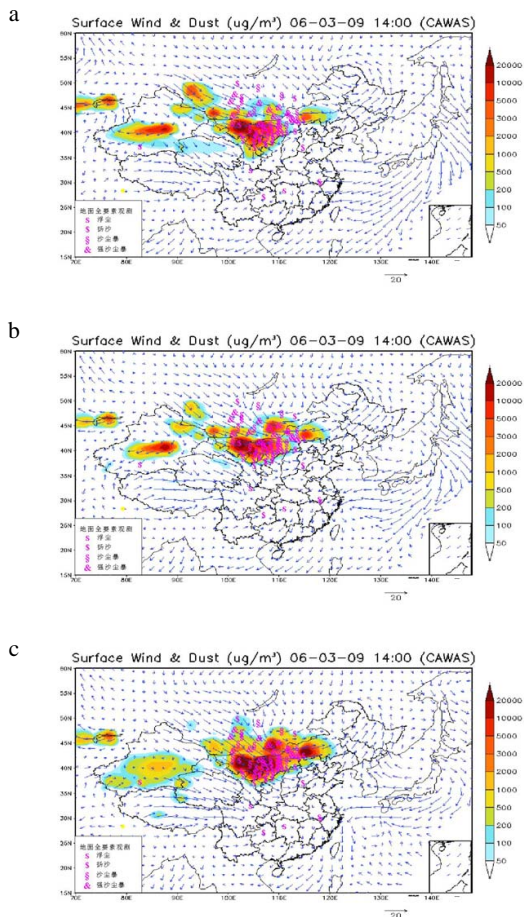
Fig. 2. Surface snap SDS concentrations and wind field at 14 h on 9 March at a forecast length of **(a)** 54, **(b)** 30 and **(c)** 6 h from the initial forecast time of 8 h on 6, 7 and 8 March, respectively (Beijing standard time used).

a

b

c
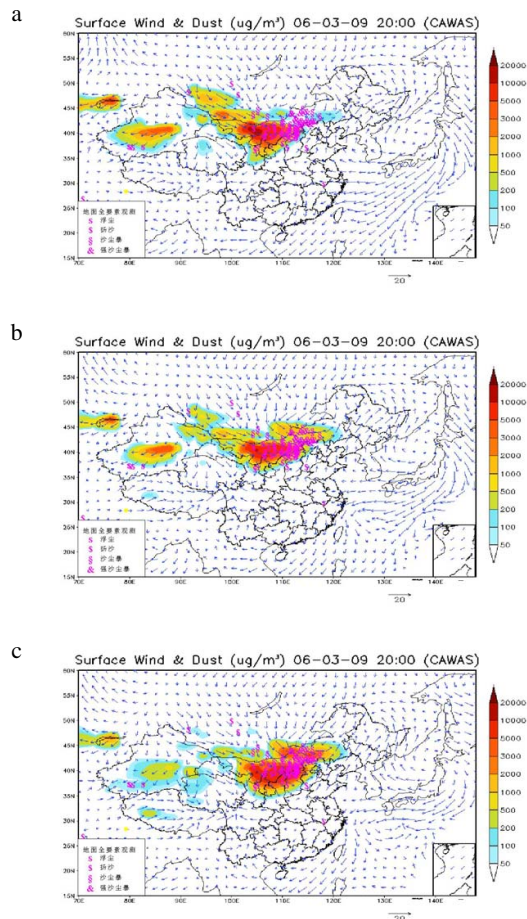
Fig. 3. Surface snap SDS concentrations and wind field at 20 h on 9 March at a forecast length of **(a)** 60 **(b)** 36 and **(c)** 12 h from the initial forecast time of 8 h on 7, 8 and 9 March, respectively (Beijing standard time used used).

Title Page

Abstract   Introduction

Conclusions   References

Tables   Figures

◄   ►│

◄   ►

Back   Close

Full Screen / Esc

Printer-friendly Version

Interactive Discussion

EGU
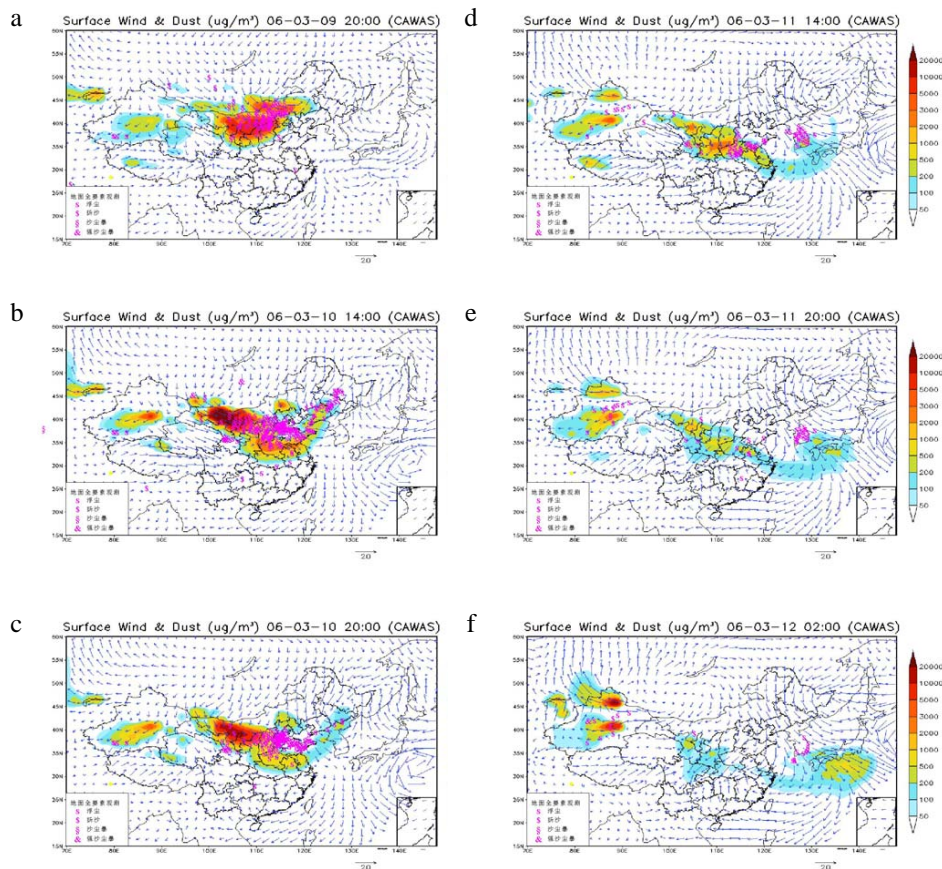
Fig. 4. Surface snap SDS concentrations and wind field at **(a)** 20 h on 9 March, **(b)** 14 hr on March 10, **(c)** 20 h on 10 March, **(d)** 14 h on 11 March, **(e)** 20 h on 11 March, and **(f)** 2 h on 12 March (local time used) from the initial forecast time of 8 h on 9 March (Beijing standard time used).
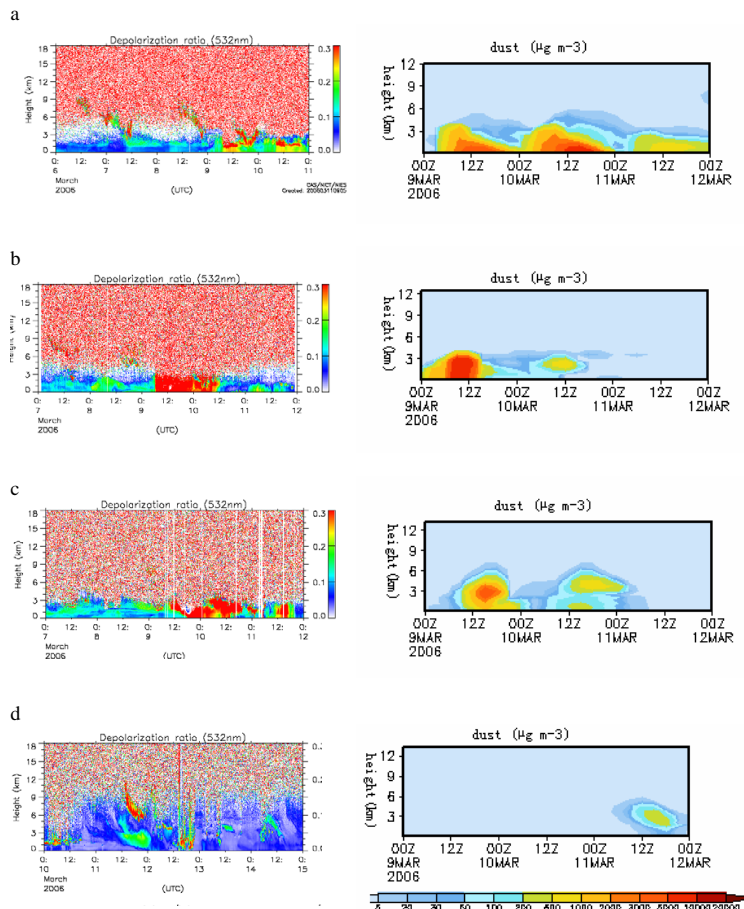
Fig. 5. Time series of lidar depolarization ratio (left) and predicted vertical concentration plot from 9 March 00:00 Z to 11 March 12:00 Z (right) for **(a)** Shapotou, **(b)** Huhhot, **(c)** Beijing and **(d)** Tskuba respectively.

Title Page

Abstract   Introduction

Conclusions   References

Tables   Figures

◄◄   ►►

◄   ►

Back   Close

Full Screen / Esc

Printer-friendly Version

Interactive Discussion
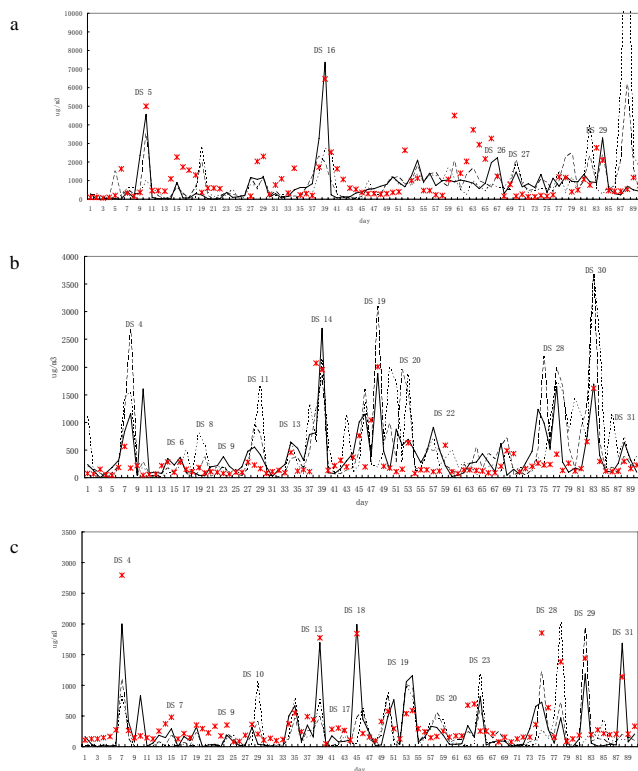
Fig. 6. Comparisons of the surface 24-h mean SDS concentration by 0–24 h (FT1), 24–48 h (FT2) and 48–72 h (FT3) forecasts and the surface PM10 observation for the entire spring from 3 March to 31 May for **(a)** Tazhong, a station in central part of Takilimakan Deserts in Xinjiang province in China, **(b)** for Ejilaqi, a station in the north of Badain Juran deserts, **(c)** for Zhurihe, a station in the west of Onqin Daga sandy areas, **(d)** for Beijing, a station away from SDS source area, and **(e)** for Dalian, a station away from SDS source areas and in the west coast of the Bohai sea, respectively. DS xx, such as DS 4, means dust event number defined in Table 1.

d

e
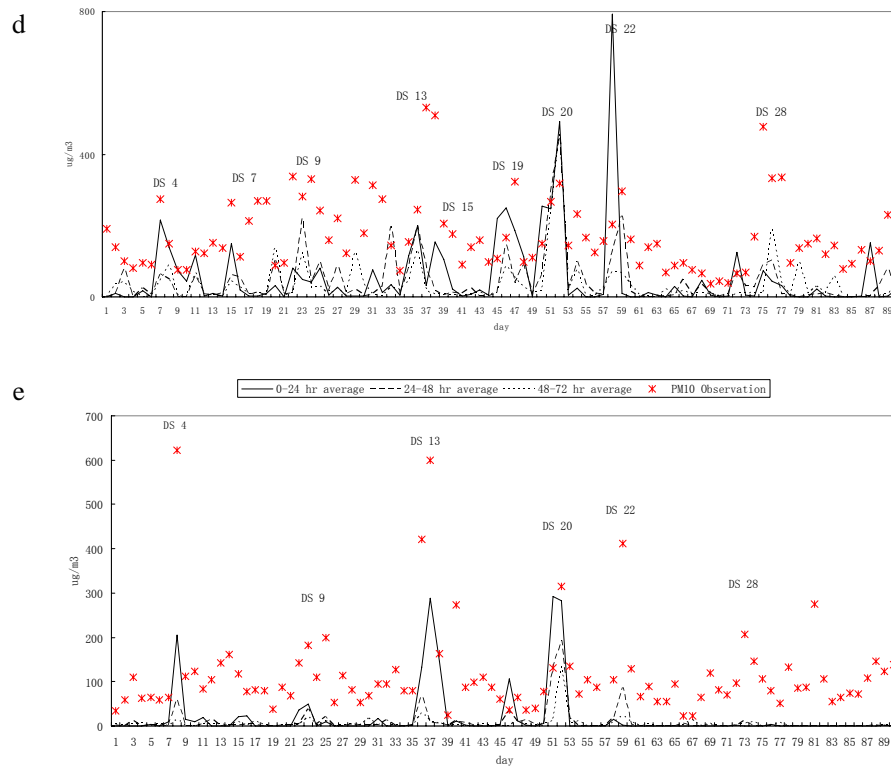
Fig. 6. Continued.

Title Page

Abstract | Introduction

Conclusions | References

Tables | Figures

|◄ | ►|

◄ | ►

Back | Close

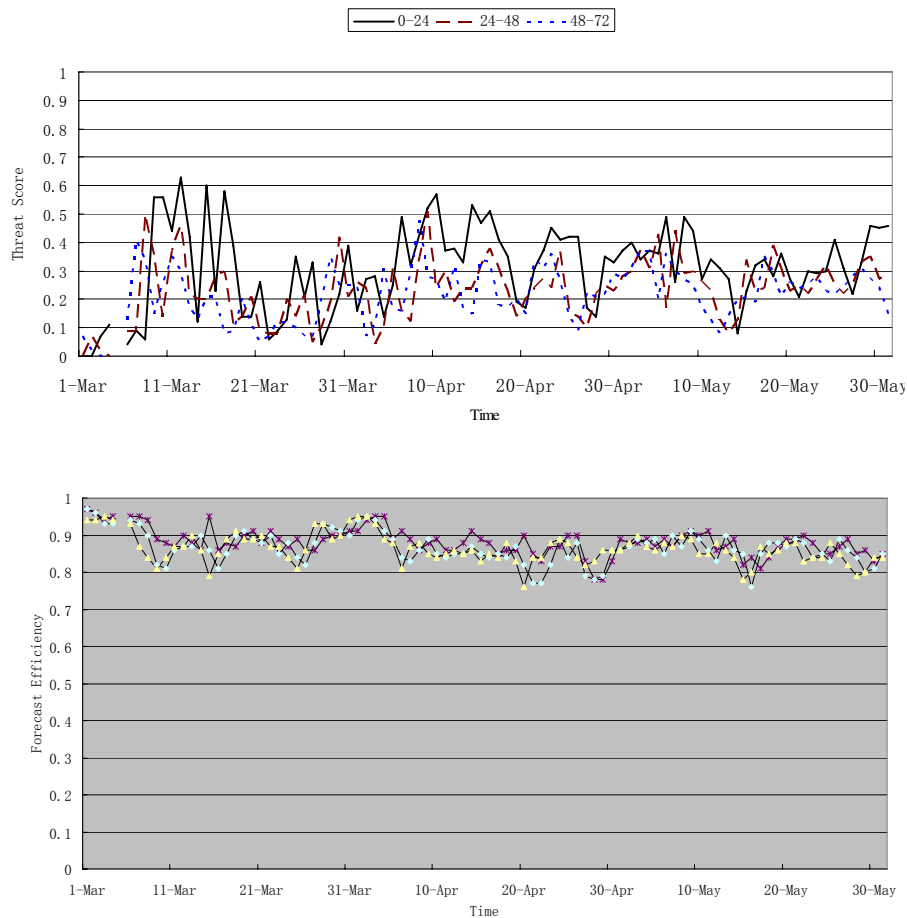Full Screen / Esc

Printer-friendly Version

Interactive Discussion

EGU

Fig. 7. Threat Scores (upper) and accuracy (lower) of 0–24 h, 24–48 h and 48–72 h forecasts for CUACE/Dust in 2006 spring.